IOP Conference Series: Earth and Environmental Science

PAPER • **OPEN ACCESS**

Retrograde Assemblages of Gneisses at Arigidi and Erusu Areas of Southwestern Nigeria

To cite this article: E. J. Oziegbe and O. Oziegbe 2023 *IOP Conf. Ser.: Earth Environ. Sci.* **1197** 012010

Retrograde Assemblages of Gneisses at Arigidi and Erusu Areas of Southwestern Nigeria

E. J. Oziegbe[1] and O. Oziegbe[2*]

1. Department of Geosciences, Faculty of Science, University of Lagos, Nigeria
2. Department of Biological Sciences, Covenant University, Nigeria ((olubukola.oziegbe@covenantuniversity.edu.ng)

Abstract

The study is aimed to unravel the presence of low-grade minerals in the migmatite terrain of Southwestern Nigeria. Mineral and textural relationship of mineral assemblages were determined using a petrographic microscope, while chemical composition was analyzed using XRF and LA-ICP-MS. Petrographic studies show the mineral assemblage, biotite + plagioclase + chlorite + epidote + quartz + muscovite + ilmenite ± calcite. There is intense alteration of both biotite and plagioclase. Textural evidence shows chloritization of biotite and epidotization of both biotite and plagioclase. Epidotization of biotite is basically at the edges of biotite while that of plagioclase in more intense at the core of grains. Primary foliation is defined by mineralogical banding of quartzo-feldspathic and mafic minerals, while secondary foliation is defined by both biotite and chlorite. SiO_2 contents are high in both gneisses (> 60 wt %), while there is a high depletion of REE. The results from field observations, mineral assemblages and textural relationship suggests that deformation due to shearing could have enhanced the retrograde chloritization of gneisses. Shearing could have created a path for the influx of fluid (H_2O & CO_2) thus triggering alteration of both biotite and plagioclase. Hydrothermal fluids containing K^+ can be said to have initiated the retrograde process which gave rise to reactions that produces secondary low grade minerals; chlorite, epidote and muscovite.

Key words: Shear zones, chloritization, epidotization, foliation, greenschist facies

1. Introduction

Several researches have over the years been carried out on the chloritization of biotite [1-8]. Chloritization can be described as a mechanism of conversion of two two layer biotite to one layer chlorite [9, 10]. Chlorite has been found to be a common accessory mineral in low-grade (greenschist facies) to medium-grade metamorphic rocks and also igneous rocks which has initial composition of ferromagnesian minerals that has undergone hydrothermal alteration [11]. Chlorite is usually unstable at temperate occurring at the surface. Chloritization of biotite gives rise to the formation of secondary minerals such as muscovite, K-feldspar, plagioclase, epidote, calcite, fluorite and Fe-oxides [12]. The breakdown of biotite has been reported to begin with the diffusion and exchange of K^+ for H^+ within biotite interlayers [4]. Biotite chloritization can take place in both hydrothermal [8, 13-15] and metamorphic [7, 16-18] environments. Chloritization of biotite can also result from the weathering process of rocks [19-21]. Weathering of migmatite can form residual soil which can be used as road pavement [22]. Such weathered rocks, as well as fractured zones, are important sources of groundwater [23, 24]. The conversion of biotite to chlorite happens when K^+ is dissociated from biotite interlayers [25]. Two different mechanisms have been identified by which biotite is hydrated to chlorite; the first is the brucitization of the interlayer [2] , while the second involves the alteration of brucite to chlorite by the brucitization of talc-like layer [26]. The structure of chloritized biotite has been studied using analytical methods such as Transmission Electron Microscopy [26, 27], Electron Microprobe [15] and X-ray diffraction (XRD). Chloritization of biotite has been reported on the mafic minor intrusive rock (diorite) from this area [28]. The area under study comprises of the highly migmatized rocks of the Basement Complex of Ikare area, Southwestern Nigeria. Previous studies [29-31] have been able to document the transition upper amphibolite to granulite facies type of metamorphism. Medium pressure and granulite temperature metamorphism has been reported for rocks (pelitic) of this region [32]. Also, retrograde assemblages have been reported in the rocks of Ikare region [32, 33]. In this study,

samples were collected from two areas of Akoko North West area of Ondo State, Southwestern Nigeria (07°35.401'N, 05° 51.311'E & 07° 34.415'N, 05° 46.603'E). The rocks under study vary from fine to coarse-grained texture and it displays a gneissose banding of millimetric separations (Figure 1a). The rocks show evidence of deformation due to the effect of shearing as seen in the contortion of foliation (Figures 1b -1d). The geological map shows that the study areas lie within the Precambrian Basement Complex (Figure 2a), and along the areas of contorted foliation within the Migmatite-Gneiss Complex (Figure 2b). In this study, we investigated the various mineral assemblage associated with chloritization processes, as well as the textural relationship to determine why low grade minerals are present in the highly migmitized rocks of Ikare area southwestern Nigeria.

2. Methodology

Thin sections were prepared and studied in detail at the labouratory of the Department of Geology, Obafemi Awolowo University. Photomicrographs of areas of interest were taken using a digital camera. Whole rock chemical analysis was carried out at the Central Analytical Facility (CAF) of Stellenbosch University, South Africa using XRF (X-ray fluorescence) and Laser Ablation Induced Coupled Plasma Mass Spectrometry (LA-ICP-MS). Using 0.7 g of the powder sample and 7 g of high purity trace element and rare earth element-free flux (LiBO2 = 32.83%, Li2B4O7 = 66.67%, LiI = 0.50%), glass discs were made for XRF analysis. Major elements were analyzed on a fused glass disc using a 2.4 kW Rhodium tube. Trace element determination was carried out using a Resonetics 193 nm Excimer laser coupled to an Agilent 7500ce ICP-MS. At a flow rate of 0.35 L/min, He gas was used for the ablation process, which was subsequently combined with argon (0.9 L/min) and nitrogen (0.004 L/min) before being introduced into the ICP plasma. Two 173 m spots were ablated on each sample for traces in fusions using a frequency of 10 Hz and 100 mJ of energy.

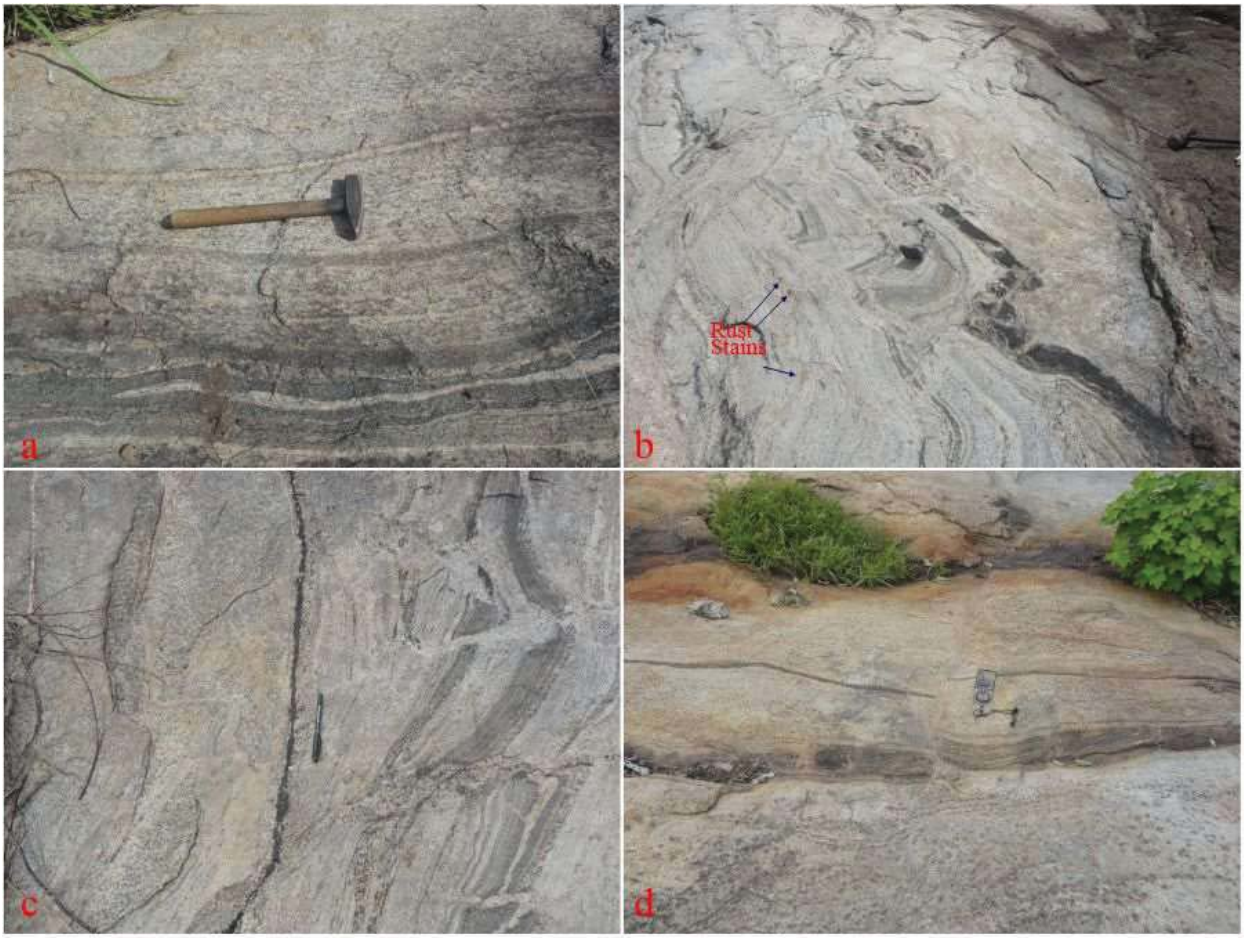

Figure 1: Field Photographs showing; a) foliated gneiss at Erusu, b) contorted and sheared foliation at Imo Arigidi, take note of the rusty stains, c) contorted and sheared foliation at Imo Arigidi, d) dragged foliation at Erusu, take note of the brownish rusty patches adjacent to fractures

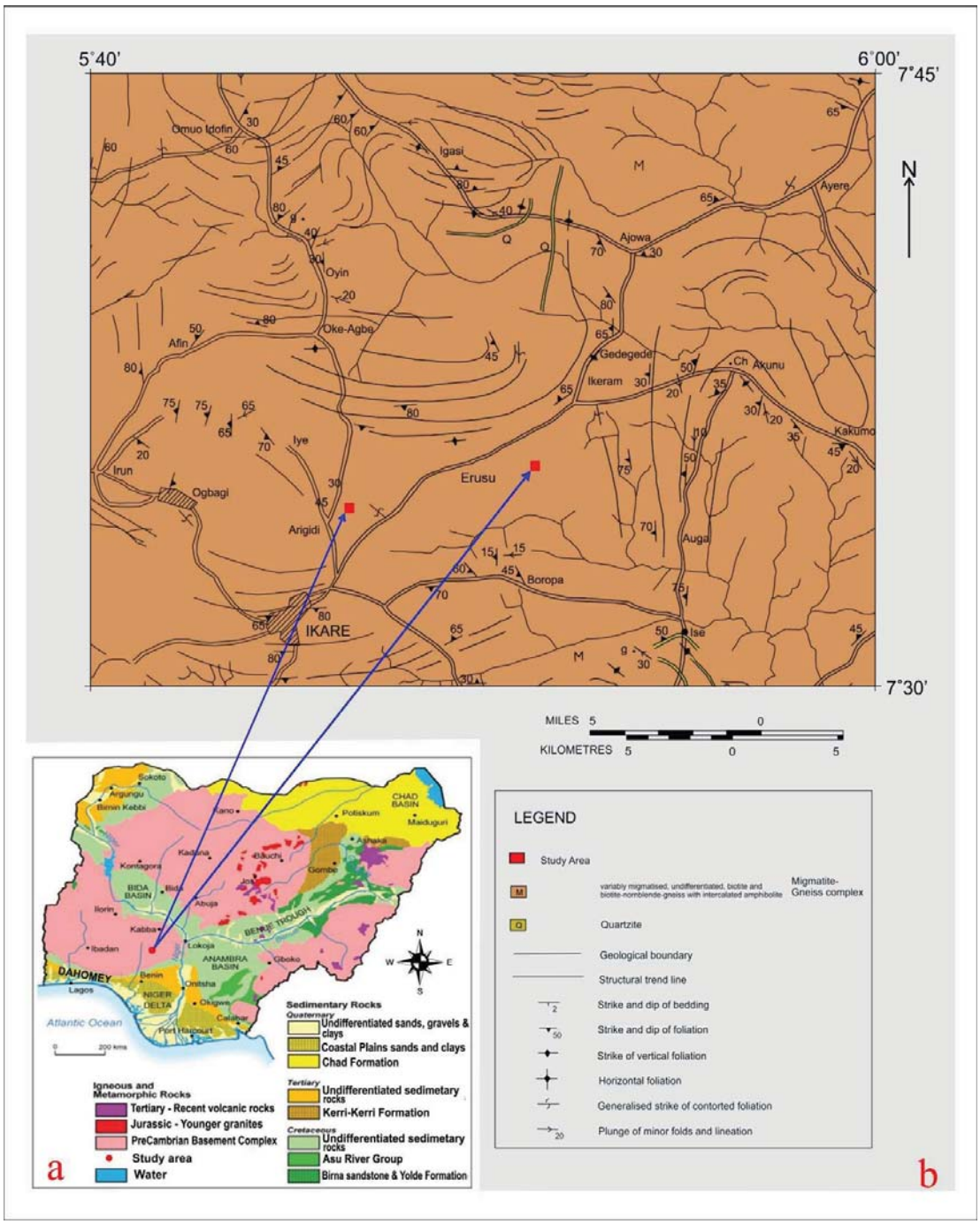

Figure 2: a) Geological settings showing the study area to be located within the Precambrian Basement Complex of Nigeria, modified after [34]. b) Geological map of Ikare region showing the study areas located along trends of contorted foliation within the Migmatite-Gneiss Complex, modified after [35].

Basaltic Hawaiian Volcanic Observatory (BHVO) glass and powder by United States Geological Survey (USGS) which are certified references were used as standards for trace element analysis [36, 37].

3. Results

3.1 Petrography

Biotite and plagioclase occur as primary minerals. Secondary minerals which include chlorite, muscovite, calcite and epidote are found on altered biotite and plagioclase (Figures 3 - 6). There is a mineralogical banding with alternation of mafic bands with quartzo-feldspathic band defining the primary foliation (Figures 3a & 3b). Most crystals of biotite are xenoblastic in nature and show a high level of alteration (Figures 3a, 3c, 3d, 4a & 4e). Chlorite appears along cleavage planes of biotite as well as around biotite (Figures 3a, 3c, 3e & 4a). There is a preferred alignment of biotite crystals defining a secondary foliation (Figures 3a & 3b). Plagioclase feldspar crystals are idioblastic to sub-idioblastic and show a high level of alteration (Figure 3f, 4b, 4c & 4d). The altered plagioclase consists of the following minerals; muscovite, epidote and calcite (Figures 3f, 4b, 4f, 5a & 5b). The alteration of plagioclase is more pronounced at the centre of the grains (Figure 4e & 4f). Plagioclase feldspar show zonation (Figures 4b & 4c). Opaque minerals (ilmenite) are mostly concentrated around grains of biotite (Figure 3c). Quartz crystals display triple junctions along grain boundaries (Figure 3f) and are closely associated with biotite epidote and plagioclase. Epidote that replaces plagioclase are colourless (Figures 4a, 4b, 4e, 4f, 6b & 6d), while epidote replacing biotite are both yellowish-green and colourless (Figures 5 & 6). Epidote grains are significantly present along cleavages and between grains of biotite (Figures 5a, 5c & 6c).

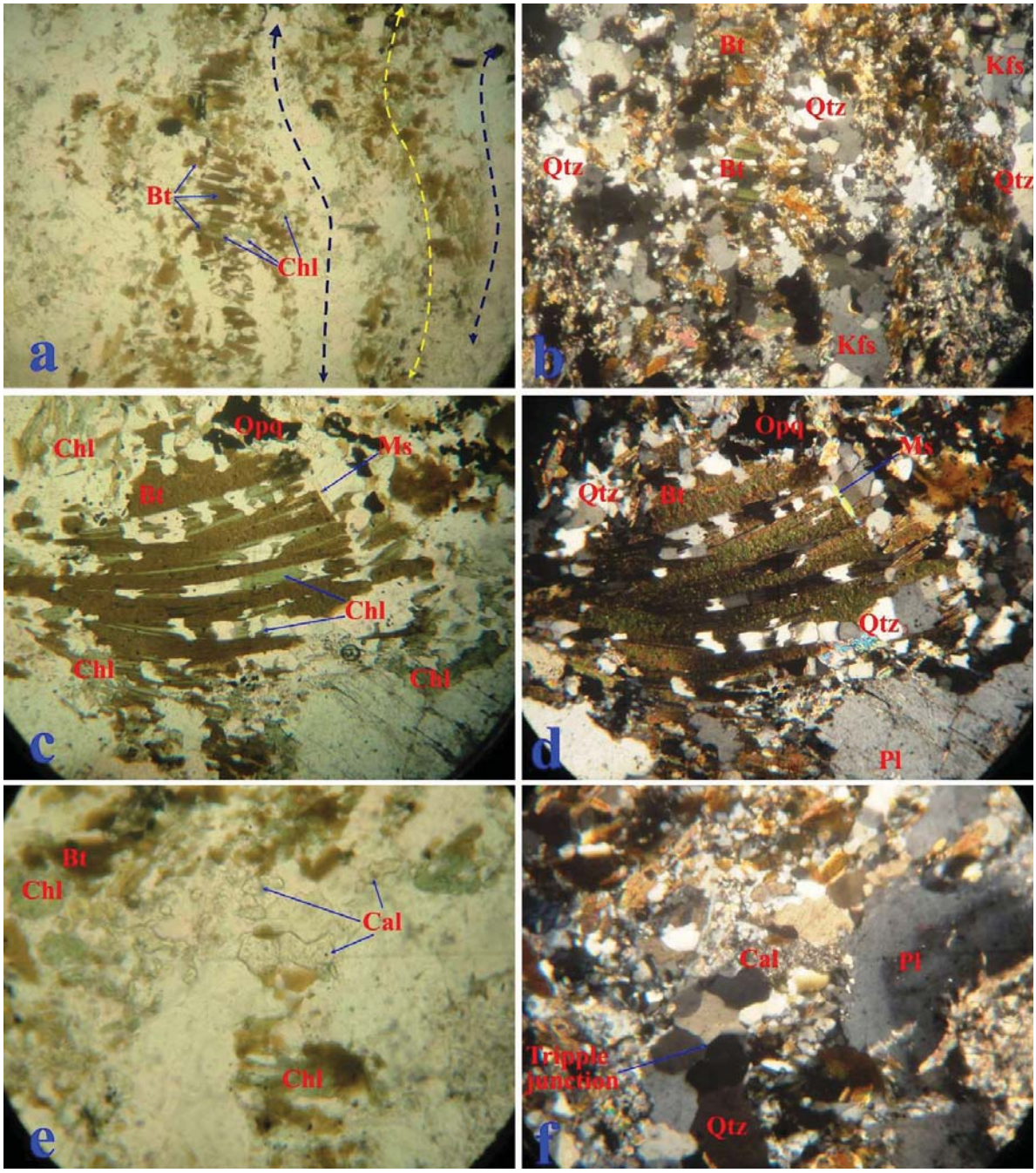

Figure 3: Photomicrographs showing; a) chlorite within cleavages of biotite, dotted lines defining foliation, PPL b) foliation defined by alternation of mafic (Bt & Chl) and felsic minerals (Qtz & Kfs), XPL c) chlorite (Chl) developing along the cleavage planes of biotite (Bt), muscovite (Ms) cuts the cleavage planes of biotite, PPL d) quartz (Qtz) and chlorite occurring in spaces created by alteration of biotite (Bt), XPL e) biotite (Bt) altering to chlorite (Chl), surrounded by calcite (Cal), PPL f) plagioclase (Pl) in close contact with calcite (Cal) and quartz, quartz (Qtz) exhibiting triple junction, XPL

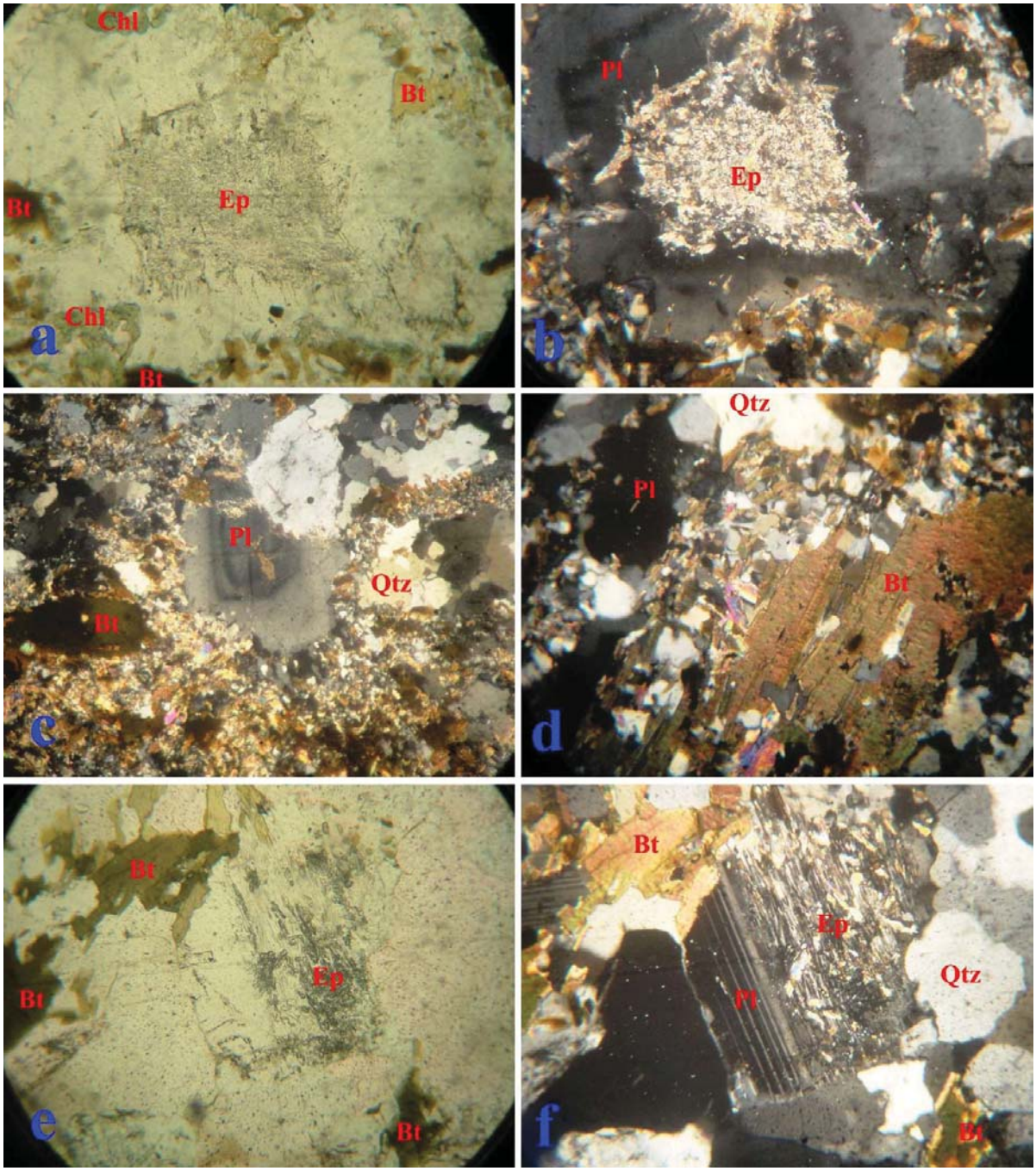

Figure 4: Photomicrograph showing; a) altered biotite (Bt), chlorite (Chl), centre dominated by colourless epidote (EP), PPL b) epidote (Ep) occurring at the centre of a zoned plagioclase (Pl), alteration occurring from core to rim, XPL c) zoned plagioclase, and the minerals quartz (Qtz) and biotite (Bt), XPL d) biotite (Bt) with K-feldspar and quartz occurring along the cleavages, quartz (Qtz) in contact with plagioclase (Pl), XPL e) greenish biotite (Bt), colourless epidote occurring at the center, PPL f) epidote (Ep) developing on plagioclase (Pl), XPL

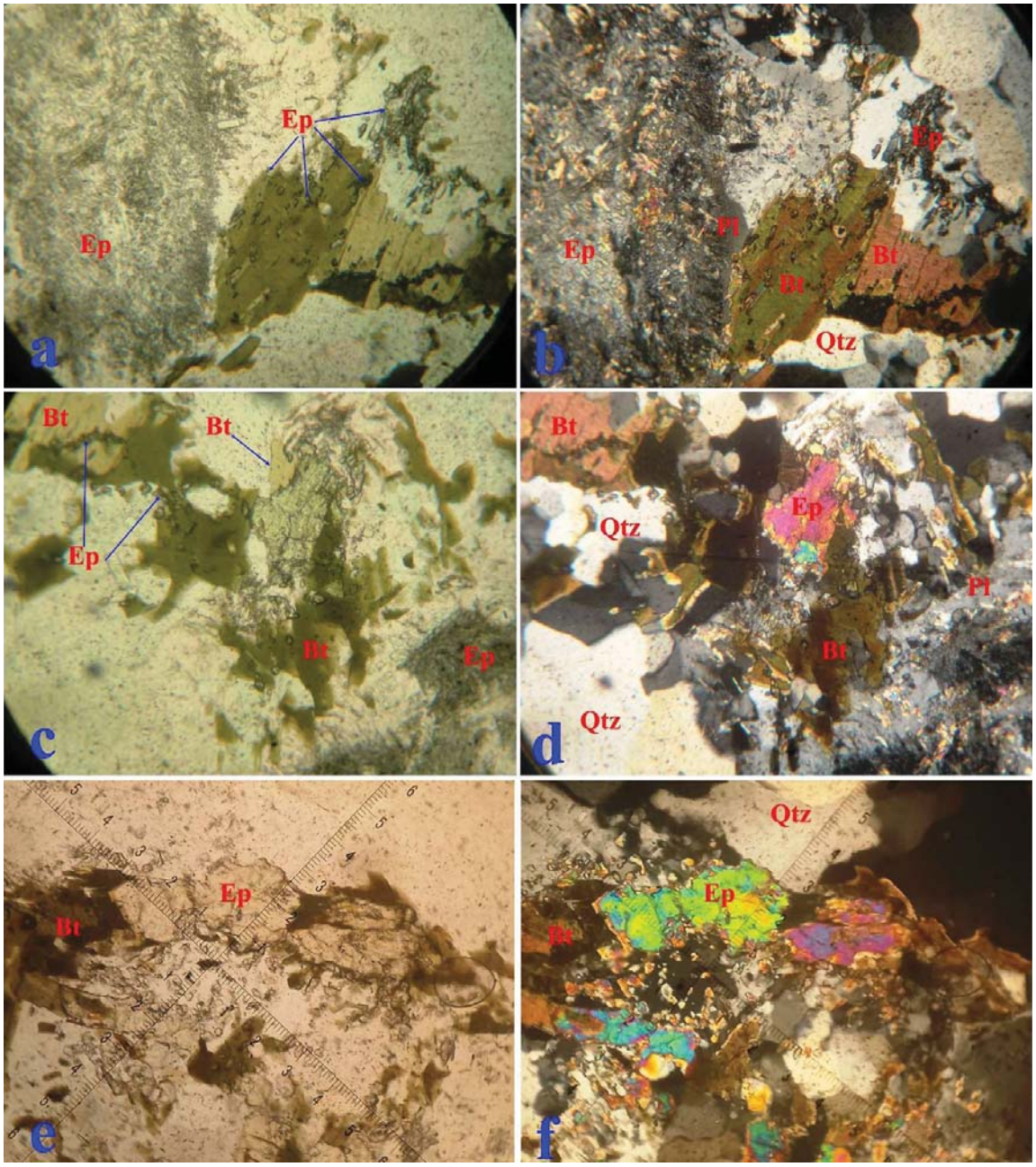

Figure 5: Photomicrographs showing; a) epidote (Ep) developing on biotite (Bt), alteration of biotite from rim to core, PPL b) epidote (Ep) developing on both plagioclase (Pl) and biotite (Bt), XPL c) green-yellow epidote (Ep) developing on greenish biotite (Bt), while colourless epidote concentrated around a colourless mineral, PPL d) quartz (Qtz) contact with biotite (Bt) epidote and plagioclase (Pl), XPL e) epidote (Ep) surrounded by biotite (Bt) grains, PPL f) epidote (Ep) surrounded by grains (Bt) and quartz (Qtz) grains, XPL

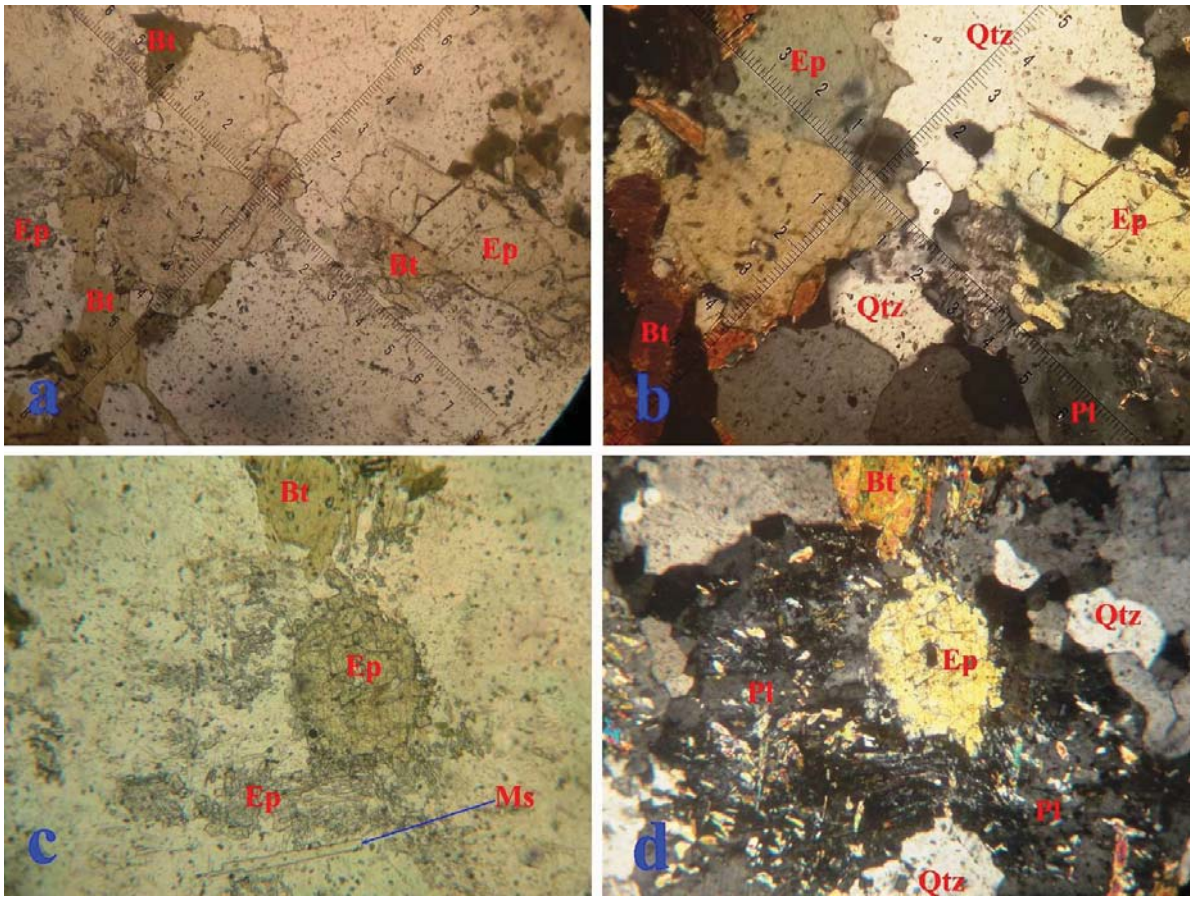

Figure 6: Photomicrographs showing; a) yellow-green epidote developing at the expense of greenish biotite (Bt), biotite (Bt) in close contact with colourless epidote (Ep), PPL, b) quartz in contact with epidote (Ep) and plagioclase feldspar (Pl), XPL c) yellowish epidote surrounded by colourless epidote (Ep), PPL d) altered plagioclase in contact with epidote (Ep) and quartz (Qtz), XPL

3.2 Geochemistry

The results of the whole rock chemical analysis are presented in Table 1. Both samples have SiO_2 content greater than 60 wt % but sample 1 has higher content of 73.69 wt % compared with sample 2 which has 61.06 wt %. Cao is higher in sample 1 (2.18 wt %) compared to sample 2 (1.62 wt %). Sample 2 has higher contents Al_2O_3 (17.82 wt %), Fe_2O_3 (5.05 wt %), K_2O (5.32 wt %) and Na_2O (6.21 wt %) compared to sample 1 with 14.04 wt %, 1.92 wt %, 3.62 wt % and 3.54 wt % respectively (Table 1). Extremely low contents were reported for TiO_2 (0.21 – 0.22 wt %) and MgO (0.28-0.54 wt %) in both samples. Sample 1 has a higher contents of V (40.95 ppm), Co (225.76 ppm), Sr (334.42 ppm) and Ba (679.61 ppm) compared to sample 2 which has 19.48 ppm, 15.32 ppm, 68.93 ppm and 212.03 ppm respectively. Rb (276.86 ppm) and Nb (514.75 ppm) contents are higher in sample 2 compared to sample 1 that has 79.29 and 2.45 respectively. Light Rare Earth Element (LREE) is enriched with respect to Heavy Rare Earth Element (HREE) in both samples, but the Rare Earth Elements contents of sample 2 is far higher than sample 1 (Table 1).

4.0 Discussion

Two sets of foliation were identified (Figures 3a & 3b), the first foliation (S_1) was defined by alternation of felsic (feldspar and quartz) and mafic (biotite and chlorite) minerals, while the secondary foliation (S_2) which is perpendicular to the S_1 is defined by biotite. These foliations could have resulted from two sets of deformation D_1 and D_2 respectively. A previous study on Ikare region had suggested at least four episodes of deformation [31], while a minimum of three themo-tectonic episodes were identified in the Okene area of the Basement Complex of Nigeria [38]. Also, Boesse and Ocan [39] in a study of high grade terrains of southwestern Nigeria have recognized two phase of deformation in southwestern Nigeria. Biotite chloritization at the shear zones have been reported in different parts of the world [7, 40-42].

Table 1: Major, trace and REE geochemistry of gneisses

Major Element	1 (wt %)	2 (wt %)	Trace Elements	1 (wt %)	2 (ppm)	REE	1 (ppm)	2 (ppm)
SiO_2	73.69	61.06	V	40.95	19.48	La	19.69	282.80
Al_2O_3	14.04	17.82	Cr	13.83	7.66	Ce	42.40	472.40
CaO	2.18	1.62	Co	225.76	15.52	Pr	4.32	43.70
Fe_2O_3	1.92	5.05	Ni	8.09	5.79	Nd	14.06	128.30
MgO	0.54	0.28	Cu	20.62	8.06	Sm	2.05	17.92
K_2O	3.62	5.32	Zn	49.84	172.35	Eu	0.78	0.70
MnO	0.02	0.07	Rb	79.29	276.86	Gd	1.30	14.37
Na_2O	3.54	6.21	Sr	334.42	68.93	Tb	0.15	2.10
TiO_2	0.22	0.21	Zr	110.20	1715.48	Dy	0.58	13.01
P_2O_5	0.07	0.06	Nb	2.45	514.75	Ho	0.11	2.71
LOI	0.32	2.16	Mo	0.64	2.04	Er	0.23	8.86
Total	100.16	99.86	Cs	0.54	0.84	Tm	0.04	1.35
			Ba	679.61	212.03	Yb	0.20	10.20
			Hf	2.83	32.56	Lu	0.05	1.55
			Ta	0.10	30.82	La_N/Yb_N	70.42	19.89
			Pb	19.51	47.63	Gd_N/Yb_N	5.36	1.17
			Th	2.87	98.86			
			U	0.32	30.63			

The geological map (Figure 2b) and field photographs are evidences that the rocks of Arigidi and Erusu (Figures 1b, 1c & 1d) have been subjected to shearing. Patches of rust stains were observed on the outcrop (Figure 1b), which might be an indication of the presence of pyrite [43], or iron oxides [44, 45] resulting from alterations of minerals within the rock. Microtexture that show high level of alteration of biotite to chlorite, epidote and muscovite (Figures 3a, 3c & 6c) can be represented by the reaction [46]:

$$\text{Plagioclase} + \text{Biotite} + H_2O \Rightarrow \text{Albite} + \text{Quartz} + \text{Muscovite} + \text{Chlorite} + \text{Epidote} \quad (1)$$

Based on the reaction above, two layered biotite is changed to single layer epidote and chlorite, while the released interlayer K^+ is used to form muscovite. The presence of epidote along the cleavages (Figures 5a) suggests that cleavages provide pathway for fluid migration during epidotization process [42]. The cutting of cleavage planes of biotite by muscovite (Figure 3c), indicates that muscovite is secondary. Alteration of biotite due to influx of fluid might have given rise to chlorite a process which has been proven to be associated with shear zones. Retrograde processes required a fluid [47, 48]. At shear zones, there could be interaction of fluids between meteoric, magmatic and metamorphic fluid, a process which is usually associated with deformation [49]. There could be a potential introduction of fluids into rocks through areas associated with brittle failure as well as through grain boundaries [50]. Chloritization during retrograde metamorphism involves the release of Si, Al and K^+, as well as a decrease in volume [9]. Biotite chloritization begins with the exchange K^+ and H^+ within the cleavages of biotite [4]. The incipient change of chlorite to biotite is commonly found in gneiss of the greenschist facies [51, 52]. Occurrence of opaque minerals such as ilmenite in the proximity of biotite (Figure 3c), is an indication that ilmenite is one of the by-products of break down of biotite [8];

$$\text{Biotite} \Rightarrow \text{Chlorite} + \text{Ilmenite} \quad (2)$$

Ilmenite in close association with altered biotite implies Ti and Fe liberated by the breakdown of biotite did not move far from the site of reaction [27]. Some Fe content are retained in chlorite while others will form opaque mineral (ilmenite). Also, presence of chloritized biotite has been linked to retrograde part of metamorphic evolution [53]. Biotite chloritization usually occur at temperature of about 600^{o}C [54]. Based on the secondary minerals, hydrothermal alteration of red stained rocks could have occurred at temperatures of between 250 – 400 ^{o}C [44]. Plagioclases show high level of alteration with some crystals exhibiting zoning structure (Figure 4b & 4c). The plagioclase is replaced by colourless epidote (Figures 4e, 4f, 5a, 6c & 6d). Through saussuritization plagioclase is altered to form epidote, chlorite and calcite [45, 55]. The saussuritization of plagioclase is more intense at the core of plagioclase crystals which are likely to have a higher anorthite content (Figures 4a). Calcite in close contact with biotite and plagioclase (Figures 3e & 3f), suggest that Ca^{2+} released from breaking down of plagioclase react with CO_3^{2-} to form carbonate [56], and can be represented by the reaction [46]:

$$\text{Plag.} + \text{Biotite} + CO_2 + H_2O \Rightarrow \text{Albite} + \text{Quartz} + \text{Muscovite} + \text{Chlorite} + \text{Calcite} \quad (3)$$

It is also important to note that transfer of products from biotite chloritization facilitates plagioclase alteration [57]. Thus, alteration of plagioclase usually occurs in the proximity of biotite chloritization [58]. The presence of triple junctions at 120^{o} among crystals of quartz are indication of equilibrium and stable arrangement (Figure 3f). The extremely low content of TiO_2 is an indication that Ti has been dissolved away. Studies has shown the mobilization of Ti and Al through distances in hydrothermal environment [59]. Low K_2O content (Table 1) might be linked to the fact that K-content of biotite is depleted during the early stages of chloritization [6]. Chloritization of biotite can lead to depletion of Cs [60] as reported for both samples (Table 1). Previous study has described retrograde assemblages in the rocks of Ikare area in which high grade mineral orthopyroxene was retrogressed to amphibole by rehydration

process [33]. The mobility of rare-earth elements may occur during the development of shear zones and migmatites [61-63], and thus could be responsible for the extremely low contents of REE in studied gneisses (Table 1).

5.0 Conclusion

The mineral assemblages in the gneisses are indicative of low-grade (i.e. greenschist) as against the granulite facies peculiar to this region and this might be due to the fact that both gneisses are located along shear zones. Intense biotite alteration as observed, could have resulted from the effect of hydrothermal fluid which was made available along the shear zones. Epidote is the most abundant alteration product of biotite and plagioclase. The concentration of epidote along cleavages of biotite is an indication that the fluid available at the shear zones flows through path ways created by cleavages in biotite. Also, altered plagioclase could have provided free Ca ions for the formation of epidote due to the close association of both altered biotite and plagioclase. Zoned plagioclase observed, might by an evidence of the precursor rock which is indicative of igneous origin.

Acknowledgment

The authors of this article are grateful to Covenant University Research, Innovation and Discovery (CUCRID) for the publication support.

References

[1] Parry, W.T. and Downey, L.M. (1982). Geochemistry of hydrothermal chlorite replacing igneous biotite. *Clays and Clay Minerals*, 30(2), pp.81-90. Doi.org/10.1346/CCMN.1982.0300201

[2] Banos, J.O. and Amouric, M. (1984). Biotite chloritization by interlayer brucitization as seen by HRTEM. *American Mineralogist*, *69*(9-10), pp.869-871.

[3] Parneix, J.C., Beaufort, D., Dudoignon, P., and Meunier, A. (1985). Biotite chloritization process in hydrothermally altered granites. *Chemical Geology*, 51(1-2), pp.89-101. Doi.org/10.1016/0009-2541(85)90089-0

[4] Eggleton, R.A. and Banfield, J.F. (1985). The alteration of granitic biotite to chlorite. *American Mineralogist*, *70*(9-10), pp.902-910.

[5] Ching-Hua, L. and Onstott, T.C. (1989). 39Ar recoil artifacts in chloritized biotite. *Geochimica et Cosmochimica Acta*, 53(10), pp.2697-2711. Doi.org/10.1016/0016-7037(89)90141-5

[6] Wilamowski, A. (2002). Chloritization and polytypism of biotite in the Łomnica granite, Karkonosze Massif, Sudetes, Poland: Stable isotope evidence. *Chemical Geology*, 182(2-4), pp.529-547. Doi.org/10.1016/S0009-2541(01)00344-8

[7] Jiménez-Millán, J., Vázquez, M., and Velilla, N. (2007). Deformation-promoted defects and retrograde chloritization of biotite in slates from a shear zone, southern Iberian massif, SE Spain. *Clays and clay minerals*, 55(3), pp.284-294. Doi.org/10.1346/CCMN.2007.0550305

[8] Yuguchi, T., Sasao, E., Ishibashi, M., and Nishiyama, T. (2015). Hydrothermal chloritization processes from biotite in the Toki granite, Central Japan: Temporal variations of

of the compositions of hydrothermal fluids associated with chloritization. *American Mineralogist*, 100(5-6), pp.1134-1152. Doi.org/10.2138/am-2015-5126

[9] Kogure, T. and Banfield, J.F. (2000). New insights into the mechanism for chloritization of biotite using polytype analysis. *American Mineralogist*, 85(9), pp.1202-1208. Doi.org/10.2138/am-2000-8-913

[10] Xiao, B. and Chen, H. (2020). Elemental behavior during chlorite alteration: New insights from a combined EMPA and LA-ICPMS study in porphyry Cu systems. *Chemical Geology*, 543, p.119604. Doi.org/10.1016/j.chemgeo.2020.119604

[11] Kohut, C.K. and Warren, C.J. (2002). Chlorites. *Soil mineralogy with environmental applications*, *7*, pp.531-553.

[12] Schwartz, G.M. (1958). Alteration of biotite under mesothermal conditions. *Economic Geology*, 53(2), pp.164-177. Doi.org/10.2113/gsecongeo.53.2.164

[13] Ferry, J.M. (1985). Hydrothermal alteration of Tertiary igneous rocks from the Isle of Skye, northwest Scotland. *Contributions to Mineralogy and Petrology*, 91(3), pp.283-304. Doi.org/10.1007/BF00413353

[14] Fiebig, J. and Hoefs, J. (2002). Hydrothermal alteration of biotite and plagioclase as inferred from intragranular oxygen isotope-and cation-distribution patterns. *European journal of mineralogy*, 14(1), pp.49-60. Doi.org/10.1127/0935-1221/2002/0014-0049

[15] Morad, S., Sirat, M., El-Ghali, M.A.K., and Mansurbeg, H. (2011). Chloritization in Proterozoic granite from the Äspö Laboratory, southeastern Sweden: record of hydrothermal alterations and implications for nuclear waste storage. *Clay minerals*, 46(3), pp.495-513. DOI: Doi.org/10.1180/claymin.2011.046.3.495

[16] Yau, Y.C., Anovitz, L.M., Essene, E.J., and Peacor, D.R., (1984). Phlogopite-chlorite reaction mechanisms and physical conditions during retrograde reactions in the Marble Formation, Franklin, New Jersey. *Contributions to Mineralogy and Petrology*, 88(3), pp.299-306. Doi.org/10.1007/BF00380175

[17] Ferrow, E.A. and Ripa, M. (1991). Chemistry, reaction mechanisms and micro-structures during retrograde metamorphism of gedrite-biotite-plagioclase bearing rocks from Bergslagen, south-central Sweden. *Lithos*, 26(3-4), pp.271-285. Doi.org/10.1016/0024-4937(91)90033-H

[18] Allaz, J., Engi, M., Berger, A., and Villa, I.M. (2011). The effects of retrograde reactions and of diffusion on 40Ar–39Ar ages of micas. *Journal of Petrology*, *52*(4), pp.691-716. Doi.org/10.1093/petrology/egq100

[19] Bisdom, E.B.A., Stoops, G., Delvigne, J., Curmi, P., and Altemuller, H.J., (1982). Micromorphology of weathering biotite and its secondary products. *Pedologie*, *32*(2), pp.225-252.

[20] Banfield, J.F. and Eggleton, R.A. (1988). Transmission electron microscope study of biotite weathering. *Clays and Clay Minerals*, 36(1), pp.47-60. Doi.org/10.1346/CCMN.1988.0360107

[21] Fordham, A.W. (1990). Treatment of microanalyses of intimately mixed products of mica weathering. *Clays and Clay Minerals*, 38(2), pp.179-186. Doi.org/10.1346/CCMN.1990.0380209

[22] Kayode, O.T. and Akinwumi, I.I. (2017). Residual soils derived from charnockite and migmatite as road pavement layer materials. *J Mater Environ Sci*, 8(2), pp.657-665.

[23] Adagunodo, T.A., Akinloye, M.K., Sunmonu, L.A., Aizebeokhai, A.P., Oyeyemi, K.D. and Abodunrin, F.O. (2018). Groundwater exploration in Aaba residential area of Akure, Nigeria. *Frontiers in Earth Science*, 6, p.66.

[24] Aizebeokhai, A.P. and Oyeyemi, K.D. (2018). Geoelectrical characterisation of basement aquifers: the case of Iberekodo, southwestern Nigeria. *Hydrogeology journal*, 26(2), pp.651-664.

[25] Xing, X.J., and Zhao, F. (2009). Biotite hydration mechanism and the influence on water injection production. *Journal of Southwest Petroleum University (Science & Technology Edition)*, 31(2), p.81. DOI: 10.3863/j.issn.1674-5086.2009.02.021

[26] Veblen, D.R. and Ferry, J.M. (1983). A TEM study of the biotite-chlorite reaction and comparison with petrologic observations. *American Mineralogist*, *68*(11-12), pp.1160-1168.

[27] Ferrow, E.A. and Baginski, B.W. (1998). Chloritisation of hornblende and biotite: a HRTEM study. *Acta Geologica Polonica*, *48*(1), pp.107-113.

[28] Oziegbe, E.J., Olarewaju, V.O., and Ocan, O.O. (2020). Mineral Chemistry And Geochemistry Of Hypersthene-bearing Diorite From Erusu Akoko, Southwestern Nigeria. *Malaysian Journal of Geosciences* (MJG), 4(1), pp.13-18. Doi.org/10.26480/mjg.01.2020.13.18

[29] Rahaman, M.A., and Ocan, O. (1988). The nature of granulite facies metamorphism in Ikare area, southwestern Nigeria. *Precambrian Geology of Nigeria, Geological Survey of Nigeria*, pp.157-163.

[30] Oziegbe, E. J. (2016). The Petrology and Geochemistry of the Basement Complex Rocks in Ikare, Oke-Agbe and Ajowa areas of Ondo State, Southwestern Nigeria. An unpublished Ph. D Thesis, Department of Geology Obafemi Awolowo University, Ile-Ife. 269p.

[31] Oyawale, A.A. and Ocan, O.O. (2020). Migmatization process and the nature of transition from amphibolite to granulite facies metamorphism in Ikare area south western Nigeria. *Journal of Geology and Mining Research*, 12(2), pp.45-64. Doi.org/10.5897/JGMR2020.0334

[32] Oziegbe, E.J., Ocan, O.O., Costin, G., and Horváth, P., (2021). Geochemistry and mineral chemistry of pelitic gneiss of Ikare area, southwestern Nigeria. *Heliyon*, 7(12), p.e08543. Doi.org/10.1016/j.heliyon.2021.e08543

[33] Oziegbe, E.J., Olarewaju, V.O., Ocan, O.O., and Costin, G. (2020). Retrogression of orthopyroxene-bearing gneiss of Iboropa Akoko, southwestern Nigeria. *Materials and Geoenvironment*, 67(3), pp.119-134. Doi.org/10.2478/rmzmag-2020-0009

[34] Oladapo, O.O., Adagunodo, T.A., Aremu, A.A., Oni, O.M. and Adewoye, A.O., 2022. Evaluation of soil-gas radon concentrations from different geological units with varying strata in a crystalline basement complex of southwestern Nigeria. *Environmental Monitoring and Assessment*, 194(7), p.486. Doi.org/10.1007/s10661-022-10173-x

[35] Dempster, A.N. (1966). 1: 250,000 Nigerian Geological Survey Sheet 61,". Geological Survey Nigeria, Akure.

[36] Jochum, K.P., Weis, U., Schwager, B., Stoll, B., Wilson, S.A., Haug, G.H., Andreae, M.O. and Enzweiler, J. (2016). Reference values following ISO guidelines for frequently requested rock reference materials. *Geostandards and Geoanalytical Research*, 40(3), pp.333-350. Doi.org/10.1111/j.1751-908X.2015.00392.x

[37] Jochum, K.P., Nohl, U., Herwig, K., Lammel, E., Stoll, B. and Hofmann, A.W. (2005). GeoReM: a new geochemical database for reference materials and isotopic standards. *Geostandards and Geoanalytical Research*, 29(3), pp.333-338. Doi.org/10.1111/j.1751-908X.2005.tb00904.x

[38] Annor, A.E. and Freeth, S.J. (1985). Thermo-tectonic evolution of the basement complex around Okene, Nigeria, with special reference to deformation mechanism. *Precambrian Research*, 28(3-4), pp.269-281. Doi.org/10.1016/0301-9268(85)90034-8

[39] Boesse, T.N. and Ocan, O.O. (1988). Geology and evolution of the Ife-Ilesha Schist belt, southwestern Nigeria. *In Symposium on Benin-Nigeria Go-traverse of Proterozoic Geology and Tectonics of High Grade Terrains* (pp. 87-107).

[40] Cheilletz, A., Ruffet, G., Marignac, C., Kolli, O., Gasquet, D., Féraud, G., and Bouillin, J.P. (1999). 40Ar/39Ar dating of shear zones in the Variscan basement of Greater Kabylia (Algeria). Evidence of an Eo-Alpine event at 128 Ma (Hauterivian–Barremian boundary): geodynamic consequences. *Tectonophysics*, 306(1), pp.97-116. Doi.org/10.1016/S0040-1951(99)00047-5

[41] Ingles, J., Lamouroux, C., Soula, J.C., Guerrero, N., and Debat, P., (1999). Nucleation of ductile shear zones in a granodiorite under greenschist facies conditions, Néouvielle massif, Pyrenees, France. *Journal of Structural Geology*, 21(5), pp.555-576. Doi.org/10.1016/S0191-8141(99)00042-5

[42] Shi, W., Wang, F., Wu, L., Yang, L., Wang, Y. and Shi, G. (2020). Geologically Meaningful 40Ar/39Ar Ages of Altered Biotite from a Polyphase Deformed Shear Zone Obtained by in Vacuo Step-Heating Method: A Case Study of the Waziyü Detachment Fault, Northeast China. *Minerals*, 10(8), p.648. Doi.org/10.3390/min10080648

[43] Leydier, T., Goncalves, P., Lanari, P., and Oliot, E. (2019). On the petrology of brittle precursors of shear zones–An expression of concomitant brittle deformation and fluid–rock interactions in the 'ductile'continental crust?. *Journal of metamorphic geology*, 37(8), pp.1129-1149. Doi.org/10.1111/jmg.12504

[44] Drake, H., Tullborg, E.L., and Annersten, H. (2008). Red-staining of the wall rock and its influence on the reducing capacity around water conducting fractures. *Applied Geochemistry*, 23(7), pp.1898-1920. Doi.org/10.1016/j.apgeochem.2008.02.017

[45] Morad, S., El-Ghali, M.A.K., Caja, M.A., Sirat, M., Al-Ramadan, K., and Mansurbeg, H. (2010). Hydrothermal alteration of plagioclase in granitic rocks from Proterozoic basement of SE Sweden. *Geological Journal*, 45(1), pp.105-116. Doi.org/10.1002/gj.1178

[46] Crawford, M.L. (1966). Composition of plagioclase and associated minerals in some schists from Vermont, USA, and South Westland, New Zealand, with inferences about the peristerite solvus. *Contributions to Mineralogy and Petrology*, 13(3), pp.269-294. Doi.org/10.1007/BF00506529

[47] Nutman, A.P., Rivers, T., Longstaffe, F., and Park, J.F.W. (1989). The Ataneq fault and mid-Proterozoic retrograde metamorphism of early Archaean tonalites of the Isukasia area, southern West Greenland: Reactions, fluid compositions and implications for regional studies. In Fluid Movements—Element Transport and the Composition of the Deep Crust (pp. 151-170). *Springer*, Doi.org/10.1007/978-94-009-0991-5_15

[48] Wintsch, R.P., Christoffersen, R., and Kronenberg, A.K. (1995). Fluid-rock reaction weakening of fault zones. *Journal of Geophysical Research*: *Solid Earth*, 100(B7), pp.13021-13032. Doi.org/10.1029/94JB02622

[49] Quilichini, A., Siebenaller, L., Teyssier, C., and Vennemann, T.W. (2016). Magmatic and meteoric fluid flow in the Bitterroot extensional detachment shear zone (MT, USA) from ductile to brittle conditions. *Journal of Geodynamics*, 101, pp.109-128. Doi.org/10.1016/j.jog.2016.05.006

[50] Cartwright, I., Power, W.L., Oliver, N.H.S., Valenta, R.K., and McLatchie, G.S. (1994). Fluid migration and vein formation during deformation and greenschist facies metamorphism at Ormiston Gorge, central Australia. *Journal of Metamorphic Geology*, 12(4), pp.373-386. Doi.org/10.1111/j.1525-1314.1994.tb00030.x

[51] McNamara, M. (1965). The lower greenschist facies in the Scottish Highlands. *Geologiska Föreningen i Stockholm Förhandlingar*, 87(3), pp.347-389. Doi.org/10.1080/11035896509448918

[52] McNamara, M.J. (1966). Chlorite-biotite equilibrium reactions in a carbonate-free system. *Journal of Petrology*, 7(3), pp.404-413. Doi.org/10.1093/petrology/7.3.404

[53] Abd El-Naby, H.H. and Frisch, W. (2002). Origin of the Wadi Haimur–Abu Swayel gneiss belt, south Eastern Desert, Egypt: petrological and geochronological constraints. *Precambrian Research*, 113(3-4), pp.307-322. Doi.org/10.1016/S0301-9268(01)00214-5

[54] Fleming, P.D. and Fawcett, J.J. (1976). Upper stability of chlorite+ quartz in the system MgO-FeO-Al2O3-SiO2-H2O at 2 kbar water pressure. *American Mineralogist*, 61(11-12), pp.1175-1193.

[55] Sandström, B., Annersten, H., and Tullborg, E.L. (2010). Fracture-related hydrothermal alteration of metagranitic rock and associated changes in mineralogy, geochemistry and degree of oxidation: a case study at Forsmark, central Sweden. *International journal of earth sciences*, 99(1), pp.1-25. Doi.org/10.1007/s00531-008-0369-1

[56] Nishimoto, S. and Yoshida, H. (2010). Hydrothermal alteration of deep fractured granite: Effects of dissolution and precipitation. *Lithos*, 115(1-4), pp.153-162. Doi.org/10.1016/j.lithos.2009.11.015

[57] Yuguchi, T., Shoubuzawa, K., Ogita, Y., Yagi, K., Ishibashi, M., Sasao, E., and Nishiyama, T. (2019). Role of micropores, mass transfer, and reaction rate in the hydrothermal alteration process of plagioclase in a granitic pluton. *American Mineralogist: Journal of Earth and Planetary Materials*, 104(4), pp.536-556. Doi.org/10.2138/am-2019-6786

[58] Eliasson, T. (1993). *Mineralogy, geochemistry and petrophysics of red coloured granite adjacent to fractures* (No. SKB-TR--93-06). Swedish Nuclear Fuel and Waste Management Co..

[59] Van Baalen, M.R. (1993). Titanium mobility in metamorphic systems: a review. *Chemical Geology*, 110(1-3), pp.233-249. Doi.org/10.1016/0009-2541(93)90256-I

[60] Gebel, A., Stosnach, H., Mengel, K., and Schmidt, K.H. (1999). Trace element analysis of granitoid minerals using laser-ablation-ICP-MS. In *Journal of Conference Abstracts* (Vol. 4, No. 1, p. 795).

[61] Lottermoser, B.G. (1992). Rare earth elements and hydrothermal ore formation processes. *Ore Geology Reviews*, 7(1), pp.25-41. Doi.org/10.1016/0169-1368(92)90017-F

[62] Rolland, Y., Cox, S., Boullier, A.M., Pennacchioni, G., and Mancktelow, N. (2003). Rare earth and trace element mobility in mid-crustal shear zones: insights from the Mont Blanc Massif (Western Alps). *Earth and Planetary Science Letters*, 214(1-2), pp.203-219. Doi.org/10.1016/S0012-821X(03)00372-8

[63] Essaifi, A., Lacinska, A.M., Corsini, M., Goodenough, K.M., Arbaoui, A.E., and Zayane, R. (2021). Mobilisation of rare earth elements in shear zones: Insights from the Tabouchent granodioritic pluton (Jebilet massif, Variscan Belt, Morocco). *Ore Geology Reviews*, 133, p.103996. Doi.org/10.1016/j.oregeorev.2021.103996